World Electric Vehicle Journal

MDPI

Article

Research on Energy Management Strategy of Fuel Cell Tractor Hybrid Power System

Sixia Zhao [1,2], Zhi Gao [1], Xianzhe Li [1], Yanying Li [1] and Liyou Xu [1,2,*]

[1] School of Vehicle and Traffic Engineering, Henan University of Science and Technology, Luoyang 471003, China; zhao_sixia@haust.edu.cn (S.Z.); 210321030294@stu.haust.edu.cn (Z.G.); 215400000018@stu.haust.edu.cn (X.L.); 220410030019@stu.haust.edu.cn (Y.L.)

[2] State Key Laboratory of Intelligent Agricultural Power Equipment, Luoyang 471003, China

* Correspondence: xlyou@haust.edu.cn

Abstract: In recent years, more and more attention has been paid to fuel cell-based hybrid tractors. In order to optimize the global power distribution of tractors and further improve the fuel economy and fuel cell durability of the system, this paper designs an energy management strategy to maximize external energy efficiency based on fuel cell/lithium battery/supercapacitor hybrid tractors. This strategy aims to reduce the real-time hydrogen consumption of the system while maximizing the external energy output so as to reduce the impact of load randomness on the output power of the fuel cell. Under the typical ploughing conditions of the tractor, the simulation is compared with the state machine strategy and the equivalent hydrogen consumption minimization strategy. The results show that the proposed strategy meets the power requirements of a given ploughing condition, and compared with the two traditional strategy systems, the performance characteristics of auxiliary energy are more fully exerted. It reduces the burden on fuel cells and improves the durability of fuel cells. The hydrogen consumption of the system was reduced by 11.03 g and 16.54 g, respectively, improving the overall economy of the hybrid system.

Keywords: hybrid tractor; fuel cell; energy management; external energy consumption

Citation: Zhao, S.; Gao, Z.; Li, X.; Li, Y.; Xu, L. Research on Energy Management Strategy of Fuel Cell Tractor Hybrid Power System. *World Electr. Veh. J.* **2024**, *15*, 61. https://doi.org/10.3390/wevj15020061

Academic Editors: Joeri Van Mierlo, Yang Luo, Tiande Mo and Yu Li

Received: 5 December 2023
Revised: 6 February 2024
Accepted: 7 February 2024
Published: 9 February 2024

1. Introduction

Due to the complex working environment, large randomness of traction fluctuation, low engine power utilization and diesel drive, traditional tractors have always had such disadvantages as high fuel consumption, poor emission and high noise [1–3]. In response to the energy transformation policy proposed by China, the agricultural machinery energy system is also gradually transitioning to clean, green and low-carbon energy systems [4,5]. Hydrogen is recognized as a secondary clean energy in the world. It has been widely used in the automotive field because of its high energy conversion efficiency, low noise, abundant reserves and renewable and water-only products [6]. Fuel cells are also suitable for tractors, and tractors have more energy storage space than cars [7]. However, when the load of the fuel cell system is abruptly changed due to the slow dynamic response speed of the compressor, the system produces an oxygen deficiency, which leads to the common problem of slow dynamic response and weak output of the fuel cell system. It is difficult to adapt to the frequent power changes during the tractor operation by using the fuel cell as the power source alone. At the same time, because of the unidirectionality of its energy conversion, the braking energy recovery cannot be realized. Therefore, the combination of fuel cells and multi-power sources is an effective way to solve this problem. The combination form is generally the integration of fuel cells with batteries or supercapacitors [8,9]. The advantage of the structure is that the auxiliary power source can provide power compensation for the fuel cell when the system load increases suddenly. On the other hand, when the load demand such as braking or deceleration is small, energy recovery can also be achieved so as to achieve the purpose of slowing down the fluctuation of fuel cell output and maximizing energy utilization [10]. In addition, although the battery has a higher power density, it has the disadvantages of low energy density, long charging time, high cost and short service life, while supercapacitors have higher energy density than traditional capacitors, higher power density than rechargeable batteries and also have fast charging and discharging and a long cycle life and are pollution-free, maintenance-free and can provide much help for batteries when used [11]. Therefore, the fuel cell plus battery plus supercapacitor topology integrates three power source characteristics: the fuel cell as the main power source to provide steady-state output, the battery as an energy buffer and the supercapacitor as a device to compensate for the sudden increase in transient power demand. For realizing the reasonable distribution of output power among multiple power sources and improving the overall efficiency of the hybrid system and the dynamic performance of the system, the multi-energy hybrid energy management strategy plays a decisive role [12]. The existing multi-energy management strategies can be divided into rule-based management strategies and optimization-based management strategies. The rule-based management strategies can be divided into deterministic rule strategies and fuzzy rule strategies. The deterministic rule strategy is to set control rules in advance according to the experience of engineering technicians or experts so as to realize the power distribution of the individual power source, which is simple, practical and feasible. Among the rules included in the strategy, the representative ones are switch control rules, power following control rules and constant temperature control rules. The fuzzy rule strategy is different from the simple switching limit of the deterministic rule strategy. It is a nonlinear control technology based on the combination of fuzzy mathematics and mathematical logic. It can predict the future driving state through fuzzy logic reasoning based on the known driving state, and it has strong robustness [13,14]. Truong et al. [15] proposed a new mapping fuzzy logic control strategy based on the fuel cell plus battery plus supercapacitor architecture. Compared with the traditional control strategy, the simulation results show that the fuel cell efficiency is improved by 47%. Based on the fuzzy logic lag state machine and differential power strategy, Peng, F and other experts [16] further proposed a processing compensation strategy, which improved the dynamic coordination efficiency between hybrid systems and increased the fuel efficiency by seven percent.

The management strategy based on optimization is to realize the optimal control of the system under the premise of setting constraints. This can be divided into global optimization control and instantaneous optimization control. The former is based on the given cycle working condition, combined with the modern optimization algorithm and control theory, in order to achieve the optimal energy distribution mode under the global cycle condition, mainly including dynamic programming control, stochastic dynamic programming and so on. The latter takes a certain working condition and driving state as the optimization interval, establishes an objective function to ensure the minimum fuel consumption in this range and optimizes the energy distribution of the system online in real time. Compared with the former, it can realize real-time dynamic optimization, mainly including Pontryagin 's minimum algorithm and equivalent consumption minimum strategy [17]. Fares, D et al. [18] proposed an offline optimization algorithm of the weighted improved dynamic programming algorithm and used a PID controller to optimize online. The results show that the algorithm converges faster than the ordinary dynamic programming algorithm, and compared with the rule-based algorithm, the fuel economy is higher. Peng et al. [19] proposed an offline optimal energy management strategy combining the Pontryagin minimum algorithm and dynamic programming algorithm, and they introduced the damping coefficient into the cost function to reduce the high dynamic oscillation of fuel cell output power. The feasibility of the strategy was verified by experiments. In addition, in recent years, the energy management strategy based on model predictive control has become the research focus of the automotive R&D industry [20]. The algorithm predicts the future driving state information of the vehicle through the prediction model, solves the local optimal problem in the finite time domain online and achieves optimal control under the whole working condition by real-time rolling optimization to achieve the global approximate optimal effect. Li et al. [21] proposed a model predictive control energy management strategy based on wavelet transform and the Levenberg–Marquardt optimized neural network. The simulation results under cyclic loading show that the algorithm has high accuracy and superiority. Li XM et al. [22] proposed an energy management strategy based on explicit model predictive control. The optimal control problem is expressed as a multi-parameter quadratic programming optimization problem, and the real-time control is realized by solving the multi-parameter quadratic programming problem offline. Compared with the traditional control strategy, the fuel economy is improved and the online calculation time is reduced.

The reasonable energy management strategy plays a decisive role in the power and economy of tractor hybrid system. Through the analysis of the existing literature, it can be found that although the rule-based energy management strategy is simple, effective and easy to implement, it depends on the given expert experience or rules, which is difficult to adapt to real-time dynamic conditions and cannot guarantee the optimal control of the hybrid system. The control strategy based on optimization has outstanding theoretical performance, which can optimize the hybrid power system to the maximum extent and improve the system performance and fuel economy. However, the strategy has high requirements on hardware and control accuracy, and the calculation time is long, resulting in high production costs and difficulties in achieving practical application. In summary, based on the fuel cell hybrid tractor, this paper proposes a strategy based on external energy efficiency maximization under the designed typical ploughing conditions, considering the tractor operating characteristics, the overall efficiency of the hybrid system and the energy utilization rate.

By analyzing the characteristics of tractor operating conditions, this paper proposes a hybrid power system suitable for tractors and mathematically models each key component of the system. Based on the idea of minimizing fuel consumption, an external energy efficiency maximization strategy is proposed. The strategy aims to ensure that the auxiliary power source is in the efficient working area while maximizing the power output, compensating the fuel cell output and maximizing the fuel cell service life and hydrogen utilization. Under the premise of maximizing the utilization rate, the global power distribution of the hybrid power system is optimized. The theoretical model is simulated by Matlab/Simulink, and the proposed strategy is compared with the traditional state machine strategy and the equivalent hydrogen consumption minimum strategy. The experimental results show that the proposed strategy is more economical and superior.

2. Design of Hybrid System

The fuel cell hybrid system structure diagram for tractors is shown in Figure 1, which is mainly composed of the fuel cell (FC), battery pack (BT), supercapacitor (SC), load motor, unidirectional DC/DC converter, bidirectional DC/DC converter DC/AC converter and energy management strategy (EMS). As the main power source, the fuel cell is connected in series with the boost unidirectional DC/DC converter and connected with the load bus to provide steady-state output power. The charge-dischargeable battery and supercapacitor are connected in series with the bidirectional DC/DC converter and connected in parallel with the fuel cell, and then connected with the load bus. The function of the energy management strategy is to reasonably dispatch the power output of fuel cells, battery packs and supercapacitors according to the real-time demand power of the load motor so as to ensure the stable operation of the system while minimizing fuel consumption. This configuration structure combines the advantages of “FC + BT” and “FC + SC” structures: it provides initial power for the tractor, compensates for the poor dynamic response performance and cold start performance of the fuel cell, realizes braking energy recovery, better absorbs or releases peak current when the load is abrupt, reduces the working pressure of the fuel cell and prolongs the cycle life of the fuel cell.

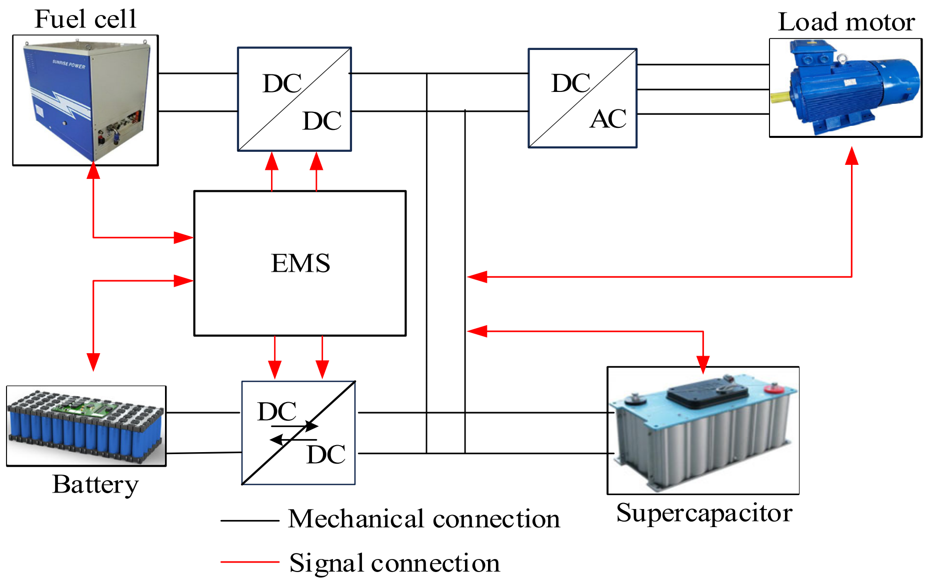

Figure 1. Schematic diagram of hybrid system.

The fuel cell hybrid tractor studied in this paper is based on a miniature agricultural multi-purpose tractor, which can tow a body, a single-sided plow, a seeder and a weeding wheel, and the main parameters are shown in Table 1.

Table 1. The main parameters of the tractor.

Parameter	Value	Parameter	Value
Standard horsepower/HP	12	Maximum horsepower/HP	15
Weight/KG	480	FC weight with hydrogen storage tank/KG	108
Battery weight/KG	19	Supercapacitor weight/KG	3.8
Motor weight/KG	117	DC/AC weight/KG	18
Size/cm	210 × 105 × 103	Drive type	Rear-wheel
Trenching depth/cm	10–20	Trench width/cm	15–20

2.1. Fuel Cell Model

The fuel cell of the model is selected to use proton exchange membrane fuel cells (PEMFCs), which are widely used in the automotive field. The equivalent circuit model is shown in Figure 2.

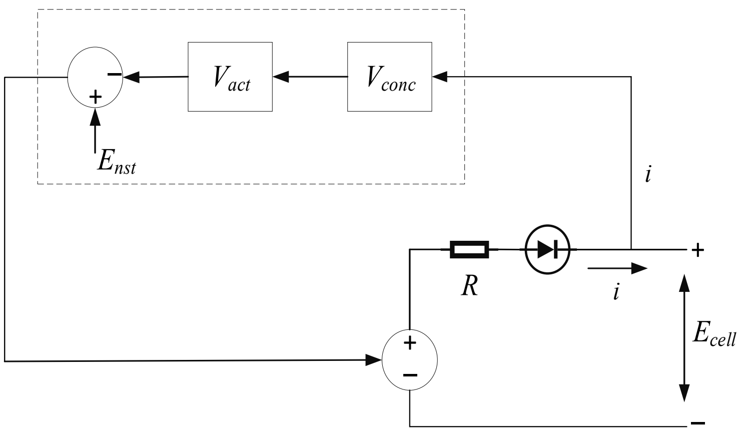

Figure 2. Fuel cell equivalent circuit model.

In a PEMFC electrochemical reaction, the output voltage will be affected by the actual working conditions, so the actual output voltage is always lower than the ideal voltage.

The output voltage loss is mainly manifested in three aspects: activation voltage loss, ohmic voltage loss and concentration voltage loss, so it can be expressed by formula [23]:

$$E_{cell} = E_{nst} - V_{act} - V_{ohm} - V_{conc}, \tag{1}$$

where E_{cell} is the net output voltage of the single PEMFC; E_{nst} is the Nernst predicted voltage; V_{act} is the activation loss voltage; V_{ohm} is the ohmic loss voltage; V_{conc} is the concentration loss voltage.

The Nernst predicted voltage can generally be expressed as follows:

$$E_{nst} = 1.229 + \frac{\Delta S}{nF}(T - 298) + \frac{RT}{nF} ln\left(P_{H_2} \cdot P_{O_2}^{0.5}\right), \tag{2}$$

where ΔS is the entropy change of the PEMFC reaction; F is the Faraday constant; T is the operating temperature of the PEMFC; R is an ideal gas constant;n is electronic mole number; P_{H_2} and P_{O_2} are the effective partial pressure of hydrogen and oxygen, respectively.

The activation loss voltage, also known as electrochemical polarization, occurs mainly at low current density discharges. The movement of electrons on both sides of the electrodes and the chemical reaction on the cathode and anode of the fuel cell cause the chemical bond breaking or formation, which requires the fuel cell to generate some energy to overcome the activation energy barrier, resulting in the loss of output voltage. The magnitude of the activation voltage loss is related to the rate of the electrochemical reaction, and the lower the reaction rate, the greater the activation voltage loss. The formula is:

$$V_{act} = \xi_1 + \xi_2 T + \xi_3 T ln C_{O_2} + \xi_4 T ln i, \tag{3}$$

where $\xi_1, \xi_2, \xi_3, \xi_4$ is the experience factor [24]; i is the current of PEMFC; C_{O_2} is the reaction concentration of oxygen in the cathode film.

The ohmic voltage loss is expressed as the potential difference between hydrogen ions as they pass through the fuel cell proton exchange membrane, electrolyte and fuel cell material, so the ohmic voltage loss depends on the fuel cell material. Charged particles are hindered during their motion, and this tendency to move forms an ohmic voltage loss. It is mainly composed of two parts, one due to the membrane impedance that prevents hydrogen ions from passing through the proton exchange membrane and the other the equivalent membrane impedance due to the internal impedance that hinders the flow of electrons through the outer circuit. The formula can be obtained by Ohm's law:

$$V_{ohm} = i\left(R_{electron} + R_{proton}\right), \tag{4}$$

where $R_{electron}$ and R_{proton} are the membrane impedance and the electron transfer impedance, respectively.

The concentration voltage loss is usually manifested as follows: due to the occurrence of electrochemical reactions, the concentration of reactants and products inside the fuel cell changes, which makes the conductivity of the liquid different and then leads to the change of the potential of the electrode, resulting in the formation of concentration voltage loss; the larger the current density, the greater the concentration voltage loss, which is described as follows:

$$V_{conc} = -\frac{RT}{nF} ln\left(1 - \frac{i}{i_{max}}\right) \tag{5}$$

where i_{max} is the limiting current of PEMFC.

The default input proton exchange membrane fuel cell has sufficient air and hydrogen flow, and the hydrogen purity is infinitely close to 100%. According to the above calculation formula and empirical formula, the PEMFC model is built on the MatlabR2021b; this is shown in Figure 3. Table 2 shows the values of the parameters entered in the model. The polarization curve of the fuel cell obtained from this model is shown in Figure 4.

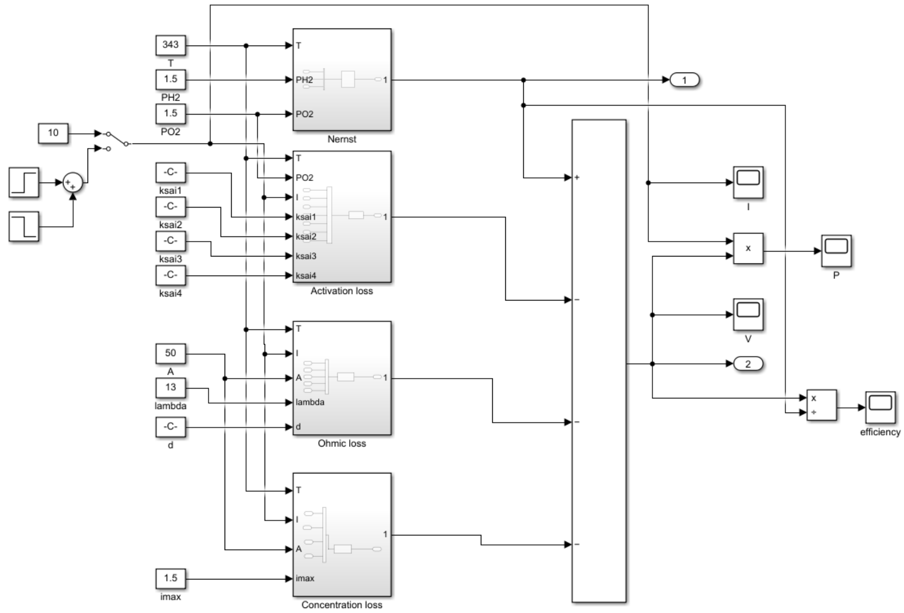

Figure 3. Simulation model of PEMFC.

Table 2. Basic parameters of the PEMFC simulation model.

Parameter	Value	Parameter	Value
$\Delta S/\mathrm{KJ}\cdot\mathrm{mol}^{-1}$	−228.57	ξ_1	−0.9514
$F/\mathrm{C}\cdot\mathrm{mol}^{-1}$	343	ξ_2	0.00312
T/K	96,485	ξ_3	-1.87×10^{-4}
$R/\mathrm{J}\cdot\mathrm{mol}^{-1}\cdot\mathrm{K}^{-1}$	8.314	ξ_4	7.4×10^{-5}
n	2	i/A	10
P_{H_2}/Pa	1.5	d/cm	0.01275
P_{O_2}/Pa	14	$A_{\mathrm{react}}/\mathrm{cm}^2$	50
λ_{H_2O}	1.5		

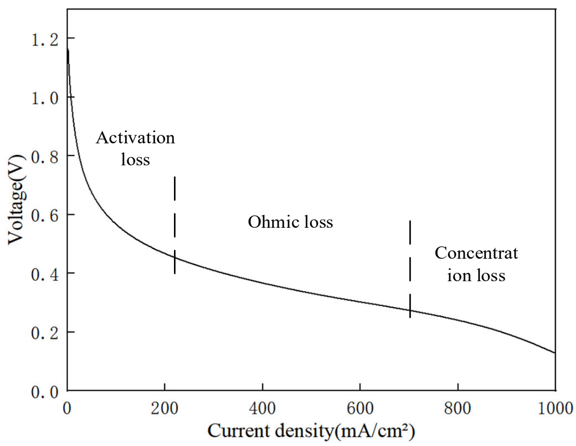

Figure 4. Fuel cell polarization curve.

The hydrogen consumption (g) of the fuel cell operating in time t can be calculated by the following equation:

$$m_{H_2}^{fc} = \int_0^t \frac{M_{H_2} N_{cell}}{2F} i(t)dt, \tag{6}$$

where M_{H_2} is the molar mass of hydrogen; N_{cell} is the number of single fuel cells; 2 is the number of electrons of hydrogen molecules.

The efficiency of the fuel cell system is calculated as follows:

$$\eta_{fc} = \frac{P_{fc}}{m_{H_2}^{fc} LHV}. \tag{7}$$

where P_{fc} is fuel cell output power and LHV is a low calorific value of hydrogen.

2.2. Power Battery Model

Compared with a lead–acid battery, nickel–cadmium battery and nickel–metal hydride battery, the power battery in this paper selects a lithium iron phosphate battery with high specific energy, high specific power, a long cycle life and good charge and discharge performance [25]. At present, many studies have proposed different lithium battery models. The most common one is the Rint model, which is equivalent to the ideal voltage source in series with the internal resistance. The ohmic internal resistance and polarization internal resistance of the battery are equivalent to a resistance R, which has the advantages of fast simulation speed and simple structure. The Shepherd model is similar to the Rint model. Figure 5 is based on the improved Shepherd model. In order to better represent the influence of the battery state of charge on the performance, the voltage polarization is added to the expression of the battery discharge voltage, that is, the internal voltage of the battery is only related to the battery state of charge and has nothing to do with the current. At the same time, in order to ensure the stable operation of the model, the filter current is used to calculate the polarization internal resistance of the battery. For this battery model, the discharge voltage is expressed by the following formula [23]:

$$V_{bat\_dis} = E_0 - K\frac{Q}{Q - A_i} i_f - K\frac{Q}{Q - A_i} A_i + Bexp(-C \cdot A_i), \tag{8}$$

where E_0 is the constant voltage for the battery; K is the polarization constant; Q is the maximum capacity of the battery; A_i is the actual battery capacity; i_f is the filtered current; B is exponential voltage; C is the exponential capacity.

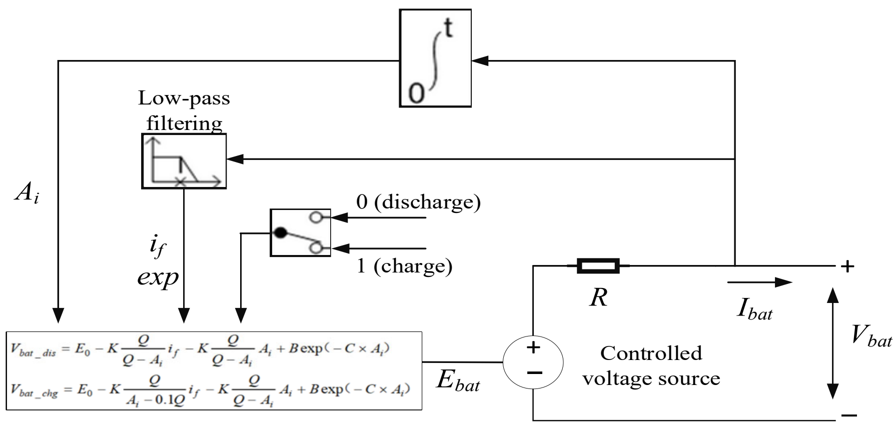

Figure 5. Lithium battery equivalent circuit model.

In the charging process, the charging voltage can be expressed by modifying the polarization resistance, which is expressed by the following formula:

$$V_{bat\_chg} = E_0 - K\frac{Q}{A_i - 0.1Q} i_f - K\frac{Q}{Q - A_i} A_i + Bexp(-C \cdot A_i), \tag{9}$$

The SOC of the lithium battery characterizes the state of charge of the battery. In order to improve the charging and discharging efficiency of lithium battery, the SOC must be maintained between 40–80%. In this paper, a simple and efficient ampere-hour integral algorithm is used to estimate the SOC of the lithium battery. The formula is as follows:

$$SOC = \frac{1}{Q}\left(Q_{in} - \frac{1}{3600}\int_0^t I_{bat}(t)dt\right). \tag{10}$$

where Q_{in} is the initial power of the lithium battery, t_0 is the initial time and I_{bat} is the lithium battery current.

2.3. Supercapacitor Model

Supercapacitors are mainly composed of two electrodes, electrolytes and porous carbon, and their advantages are high power density, fast charging speed and the ability to store and release more energy, which is complementary to the performance characteristics of lithium batteries. The commonly used supercapacitor models include the classical equivalent model, artificial neural network model and electrochemical model. The classical equivalent model has a simple circuit structure and relatively simple calculation and analysis of related parameters, but the calculation accuracy is relatively low because the model does not consider the nonlinear characteristics of supercapacitors. The artificial neural network model can more accurately represent the nonlinear characteristics of supercapacitors, but the accuracy of the model depends on the quantity and quality of training data, the practical application value is low and the application scope is too narrow. Electrochemical models can use partial differential equations to accurately describe the internal workings and changes of supercapacitors. Based on this, the supercapacitor model adopted in this paper is a Stern-based electric double-layer electrochemical model, as shown in Figure 6, which integrates the Helmholtz and Gouy–Chapman models [26]. Stern divides the electric double-layer capacitance of supercapacitors into compact layer capacitors and diffusion layer capacitors that are tightly adsorbed on the solid surface and reasonably explains the electrokinetic phenomenon; the capacitance of the supercapacitor model can be expressed as:

$$C = \left[\frac{l}{N_e \tau \tau_0 A} + \frac{2N_e RT}{FQ_c sinh\left(\frac{Q_c}{N_e^2 A\sqrt{8RT\tau\tau_0 c}}\right)}\right]^{-1}, \tag{11}$$

where N_e is the number of electrode layers; τ and τ_0 are the dielectric constants of electrolyte materials and free space, respectively; A is the contact area between the electrode and the electrolyte; l is the length of the Helmholtz layer; Q_c is the supercapacitor charge; F is the Faraday constant; R is an ideal gas constant; T is the operating temperature; c is the molar concentration.

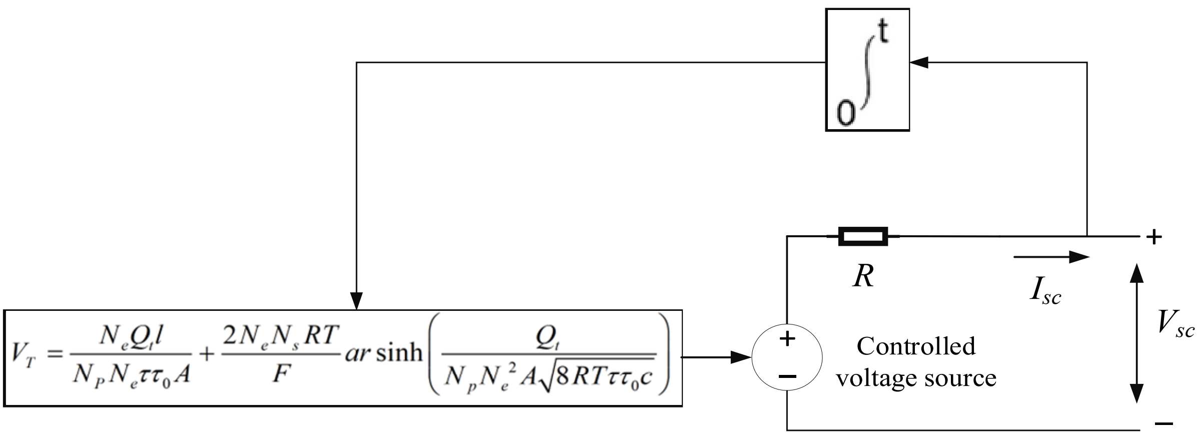

Figure 6. Supercapacitor equivalent circuit model.

The total capacitance of the supercapacitor can be expressed as follows:

$$C_t = \frac{N_p}{N_s} C, \tag{12}$$

where N_p and N_s are the number of series and parallel connections in the supercapacitor module, respectively.

The output voltage of the supercapacitor can be expressed by the Stern equation as follows:

$$\begin{cases} V_{sc} = \frac{Q_t}{C_t} - R_{sc} \cdot I_{sc} \\ Q_t = N_p Q_c = \int_0^t I_{sc}(t)dt \end{cases}. \tag{13}$$

where Q_t, R_{sc} and I_{sc} are the total charge, resistance and current of the supercapacitor module, respectively.

2.4. DC/DC Converter Model

The terminal voltages of the fuel cells, lithium batteries and supercapacitor are lower than the voltage required to supply power to the load. Therefore, the fuel cell and the unidirectional step-up DC/DC converter are connected in series to the load bus to increase the output voltage of the fuel cell. In the case of high-frequency fluctuation of load power demand, the stable power output of the fuel cell system is maintained [27]. The lithium battery and supercapacitor are connected in series with a bidirectional buck-boost DC/DC converter, and then connected to the load bus, so as to achieve the effect of charge and discharge. During the charging process, the energy flows from the motor or fuel cell to the auxiliary power source to maintain the auxiliary power source SOC in the high-efficiency range, and during the discharge process, the energy flows from the auxiliary power source to the load motor to provide power compensation for the fuel cell. In order to reduce the computational burden, this paper adopts the average DC/DC converter model [28] and directly controls the duty cycle without using the pulse width modulation strategy. As shown in Figure 7, they are a unidirectional boost DC/DC converter circuit and bidirectional DC/DC converter circuit, respectively. In addition, both DC/DC converters use current feedback control to control the output power of each power source by adjusting the current of the DC/DC converter.

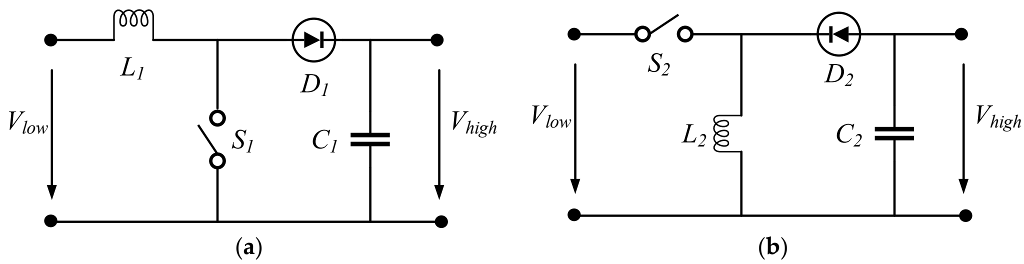

Figure 7. (**a**) Unidirectional DC/DC converter circuit; (**b**) bidirectional DC/DC converter circuit.

2.5. DC/AC Inverter Model

The DC/AC inverter is mainly composed of diodes, thyristors, capacitors and reactances, and the function is to use the control of each component to invert the DC output of the hybrid system into a three-phase alternating current for asynchronous motors. During normal driving, the inverter adjusts the output torque of the traction motor by controlling the amplitude and frequency of the three-phase alternating current; during braking downhill, the alternating current fed back by the traction motor can also be inverted into a direct current to charge the auxiliary energy. According to the nature of DC power supply, DC/AC inverters can be divided into current-type and voltage-type inverters. Among them, the voltage inverter is also divided into two-point and three-point structures. The three-point structure output voltage harmonic component is lower and the control accuracy is higher, but the structure is relatively complex. The structure and control of the two-point inverter are relatively simple, and the output voltage harmonic composition is acceptable for the tractor hybrid system. Therefore, a voltage-type three-phase full-bridge two-point DC/AC inverter is used, and its equivalent circuit is shown in Figure 8.

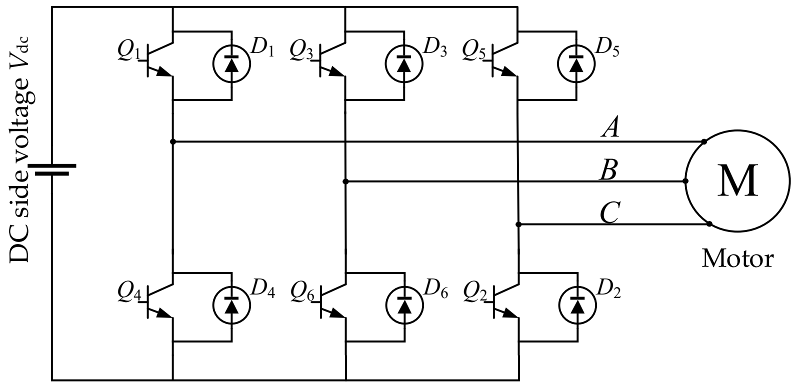

Figure 8. Voltage type three-phase full-bridge two-point DC/AC inverter.

2.6. DC/DC Converter Model

A motor is a device that converts electrical energy and mechanical energy into each other. Considering that the research focus of this paper is the research on the energy management strategy of hybrid power systems, in order to avoid the over-complexity of the motor model controller and speed up the simulation time, the three-phase AC load model built in Matlab/Simulink will be used in this paper, as shown in Figure 9. Its advantage is that it has a large torque output and high operating efficiency, and it can also be used for inverter control to realize the control of motor start and stop and frequency conversion speed regulation, which is very suitable for the operation characteristics of tractors.

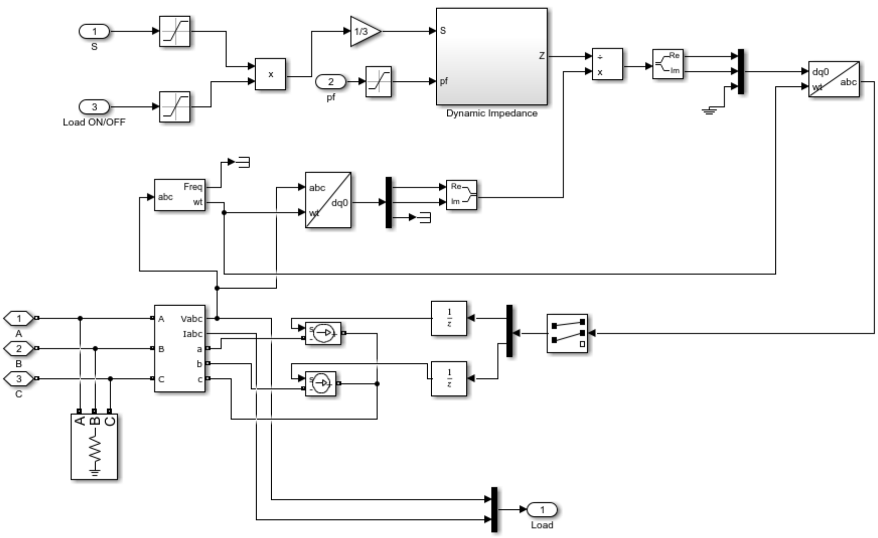

Figure 9. Simulation model of a 3-phase asynchronous motor.

3. Hybrid Energy Management Strategy

The essence of an energy management strategy is to allocate the output power of the fuel cell, battery and supercapacitor to ensure that the system is operating optimally. Therefore, when designing an energy management strategy, in addition to considering the overall physical model of the system, it is also necessary to consider the working characteristics of each component of the system, so that each component is approximately in the efficient working area, so as to improve the overall performance of the hybrid system.

The design of the fuel cell hybrid tractor energy management strategy should follow the following objectives:

(1) Motivation first

It should be ensured that the tractor has enough driving force in the normal driving or operation process and at the same time ensure the stability and safety of the operation so as to design a reasonable control strategy and improve the economy of the system.

(2) Fuel cell drive is preferred

The fuel cell hybrid system designed in this paper is based on the fuel cell as the main power source, providing the main power output for the system, and the lithium battery and supercapacitor as the auxiliary power source to provide buffering and power compensation for the fuel cell.

(3) Improve the durability of fuel cell

Due to the high cost of fuel cell use, from an economic point of view it is necessary to consider improving the durability of fuel cells, avoiding frequent fluctuations in fuel cell output power and ensuring long-term high-potential operation.

(4) Good applicability

The designed energy management strategy should have good dynamic performance, adaptive ability and be able to be applied to more working conditions; it should also adapt to the randomness of complex working conditions without changing its design parameters and ensure the good economy of the system on this basis.

3.1. State Machine Control Strategy (SMC)

SMC is a traditional control strategy based on deterministic rules. It can determine the output of the controller simply and reliably according to the preset rules, which has the advantages of small calculation and online implementation. According to the structural characteristics of the ternary hybrid system designed in this paper, combined with the load and working condition characteristics of the tractor, the SMC suitable for the system is constructed. The control strategy is shown in Figure 10 [29]. ①–⑧ are the rules in the eight states of the strategy, * stands for reference output parameter. The lithium battery SOC and the load demand power are selected as the primary input variables. According to the performance characteristics of each power component, the upper and lower limits of the battery SOC, the charging power and the upper and lower limits of the fuel cell output power are set to obtain the reference output power of the fuel cell. The reference value is converted into a current signal for control, thereby determining the working mode of the hybrid power system and ensuring that the power system is in an efficient working range.

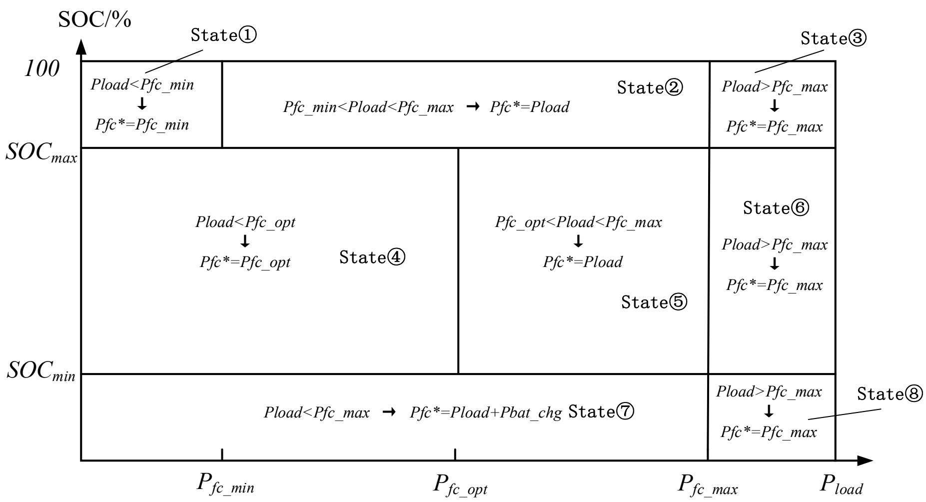

Figure 10. Block diagram of SMC configuration scheme.

3.2. Equivalent Hydrogen Minimum Strategy (ECMS)

ECMS is a short-term equivalent fuel consumption optimization strategy based on the Pontryagin Minimum Principle (PMP), which aims to equate the power consumption of the energy storage power source with the hydrogen consumption while the energy source runs smoothly and transform the global optimization problem into an instantaneous optimization problem with the smallest equivalent hydrogen consumption at a certain time, so as to minimize the total hydrogen consumption of the hybrid system. Then, the equivalent hydrogen consumption of the lithium battery in a sampling time is expressed as:

$$J_{min} = m_{H_2}^{fc}(t) + m_{H_2}^{bat}(t) + m_{H_2}^{sc}(t) \tag{14}$$

where $m_{H_2}^{fc}$ is fuel cell hydrogen consumption; $m_{H_2}^{bat}$ is the equivalent hydrogen consumption of lithium batteries; $m_{H_2}^{sc}$ is the equivalent hydrogen consumption of supercapacitors.

Since the DC bus voltage is controlled by the DC/DC converter, the supercapacitor will be charged with the same energy as the lithium battery after discharge, and the equivalent energy consumption of the supercapacitor is used to compensate for the power fluctuation of the system, which is equivalent to the power demand of the load handled by the fuel cell and lithium battery alone. The energy supply and working time of the supercapacitor account for a small proportion of the whole cycle condition, and the hydrogen consumption of the supercapacitor is small compared with the hydrogen consumption of the fuel cell and the equivalent hydrogen consumption of the lithium battery, so it is negligible in the steady-state situation [30]. The cost function of ECMS can be rewritten as follows:

$$J_{min} = m_{H_2}^{fc}(t) + m_{H_2}^{bat}(t) \tag{15}$$

The block diagram of the ECMS scheme is shown in Figure 11 [31]. The implementation principle refers to the equivalent factor k and the lithium battery electrical energy is equivalent to hydrogen consumption; then, the equivalent hydrogen consumption of the lithium battery in a sampling time is expressed as:

$$m_{H_2}^{bat}(t) = \begin{cases} \int_0^t k(t)\frac{P_{bat}(t)}{\eta_{bat}LHV}, P_{bat}(t) \geq 0 \\ \int_0^t k(t)\frac{P_{bat}(t)\eta_{bat}}{LHV}, P_{bat}(t) < 0 \end{cases}, \tag{16}$$

where P_{bat} is the lithium battery power; η_{bat} is lithium battery efficiency. The specific optimization cost function of ECMS is expressed as:

$$J_{min} = m_{H_2}^{fc}(t) + m_{H_2}^{bat}(t) \tag{17}$$

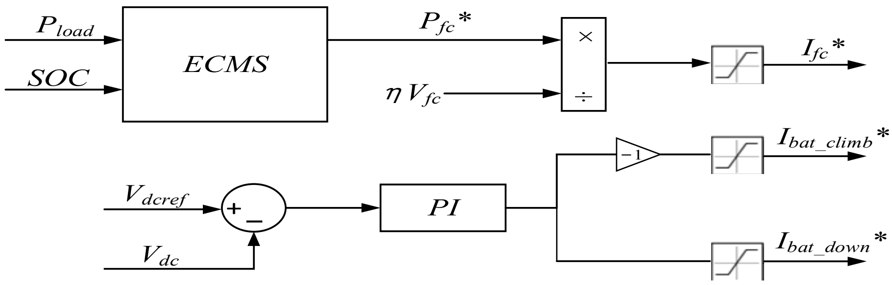

Figure 11. Block diagram of ECMS configuration scheme.

Among them, the equivalent factor is the core of the ECMS strategy, which is extremely sensitive to working conditions, and the wrong selection will lead to large or small final SOC of lithium batteries and low system efficiency. Therefore, it is necessary to control the SOC of lithium batteries in the efficient working area to reduce the sensitivity of ECMS to the SOC balance coefficient. The equivalent factor expression is shown in Equation (18), and the problem is constrained by the equation and boundary of Equation (19).

$$k = 1 - 2\mu \frac{[SOC - 0.5(SOC_{max} + SOC_{min})]}{SOC_{max} + SOC_{min}} \tag{18}$$

$$\begin{cases} P_{load} = P_{fc} + P_{bat} \\ P_{fcmin} \le P_{fc} \le P_{fcmax} \\ P_{batmin} \le P_{bat} \le P_{batmax} \\ 0 \le k \le 2 \end{cases} \tag{19}$$

where P_{fc}, P_{bat} and P_{load} are the output power of the fuel cell and lithium battery and the load demand power, respectively; k is the equivalent factor; ΔT is the sampling time; μ is the balance coefficient of SOC for lithium battery; SOC_{max} and SOC_{min} are the upper and lower limits of the lithium battery SOC, respectively; P_{fcmax} and P_{fcmax} are the upper and lower limits of fuel cell output power, respectively; P_{batmax} and P_{batmin} are the upper and lower limits of lithium battery output power, respectively.

3.3. External Energy Efficiency Maximization Strategy (EEMS)

In the "FC + BT + SC" hybird, EEMS aims to maximize the output power of the lithium battery and supercapacitor while maintaining the battery SOC in the normal range and minimize the cumulative hydrogen consumption of the system, thereby improving the overall fuel economy of the system [32]. Moreover, the cost function of the algorithm does not need to evaluate the equivalent battery energy, and the calculation is relatively simple.

The power allocation problem of the fuel cell tractor hybrid system studied in this paper belongs to a nonlinear optimization problem under a series of soft constraints. The state space equation of the system at a certain moment can be expressed as:

$$\dot{x}(t) = f(x(t), u(t)), \tag{20}$$

where $x(t)$ is the state variable; $u(t)$ is the control variable; t is a time variable; $f(x(t), u(t))$ is a continuous differentiable function about $x(t)$ and $u(t)$.

$$x = \begin{bmatrix} P_{bat} \\ \Delta V \end{bmatrix}, u = \begin{bmatrix} SOC \\ V_{dc} \end{bmatrix}, \tag{21}$$

where P_{bat} is the output power of the lithium battery in the sampling time; ΔV is the charge and discharge voltage of the supercapacitor; SOC is the initial state of charge of the lithium battery; V_{dc} is the DC bus voltage.

In order to reduce the amount of calculation and improve the speed of solution, the nonlinear problem is approximately linearized to obtain a new linear time-varying state equation, as shown below:

$$\dot{\widetilde{x}}(t) = A\widetilde{x}(t) + B\widetilde{u}(t), \tag{22}$$

$$A = \begin{bmatrix} \Delta t & 0 \\ 0 & -1 \end{bmatrix}, B = \begin{bmatrix} (u_1(t) - SOC_{min}) \cdot V_{bat\_nom} \cdot Q \\ u_2(t) - V_{dc\_min} \end{bmatrix}, \tag{23}$$

where V_{bat_nom} is the rated voltage of the lithium battery; Q is lithium battery capacity. The initial state is as follows:

$$x(0) = \begin{bmatrix} P_{bat\_max} \\ V_{dc\_min} \end{bmatrix}. \tag{24}$$

The process of the EEMS control scheme is shown in Figure 12 [33]. The input is the initial SOC and DC bus voltage of the lithium battery, and the output is the reference power of the lithium battery and the charge and discharge voltage of the supercapacitor. The reference power of the lithium battery is compared with the load demand power, and the reference power of the fuel cell is estimated by the obtained fuel cell current. The charge and discharge state of the battery is evaluated by comparing the sum of the DC bus voltage and the supercapacitor charge and discharge voltage with the reference DC bus voltage. The core of the energy management strategy to solve the optimal control problem is to minimize the overall hydrogen consumption of the system. In the EEMS optimization algorithm, the two variables of lithium battery power and supercapacitor charge and discharge voltage need to be evaluated, aiming to find the optimal solution. The cost function provides the maximum energy for the lithium battery and supercapacitor within a certain time interval. The formula is as follows:

$$J_{max} = -\left(P_{bat}\Delta T + \frac{C_{sc}\Delta V^2}{2}\right) \tag{25}$$

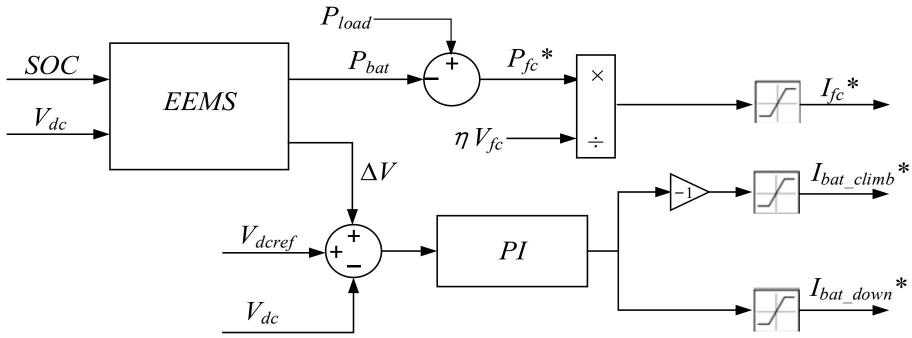

Figure 12. Block diagram of EEMS configuration scheme.

And the optimization process is subject to the following inequality constraints:

$$P_{bat}\Delta T \leq (SOC - SOC_{min})V_{bat}Q_{bat} \tag{26}$$

The boundary conditions are as following:

$$\begin{cases} P_{bat\_min} \leq P_{bat} \leq P_{bat\_max} \\ V_{dc\_min} \leq V_{dc} \leq V_{\backslash dc\_max} \end{cases} \tag{27}$$

where C_{sc} is the rated capacity of the supercapacitor; V_{bat} and Q_{bat} are the voltage and capacity of lithium battery; P_{bat_max} and P_{bat_min} are the maximum and minimum values of the output power of the lithium battery, respectively; V_{dc_max} and V_{dc_min} are the maximum and minimum values of DC bus voltage, respectively.

In summary, by evaluating the optimal solution in the control time domain, EEMS makes the optimal solution have a maximum value in the whole control time domain, which is equivalent to the minimum value of the overall hydrogen consumption of the system. Therefore, this strategy becomes an effective method to solve the optimal power allocation problem of the tractor hybrid system.

4. Simulation and Results Analysis

In order to verify the effectiveness and advantages of the energy management strategy designed in this paper, the basic parameters of the main components of the hybrid power system are set up, and the simulation scheme is built in the Matlab/Simulink simulation environment. Under the typical load conditions of the tractor, the performance of the hybrid power system is analyzed according to the simulation output results.

4.1. Load Condition Setting

Unlike automobiles, agricultural tractors are mainly used in soft soil in the field, with poor road conditions, low speed and serious slippage, and are generally used for ploughing, rotary tillage, sowing, transportation and other operations. Based on the miniature tractor, the working condition of the tractor pulling the single-sided plough for a ploughing operation is selected as the system input, and its running trajectory is mainly based on straight and U-turn, as shown in Figure 13, and the arrow indicates the trajectory of the tractor.

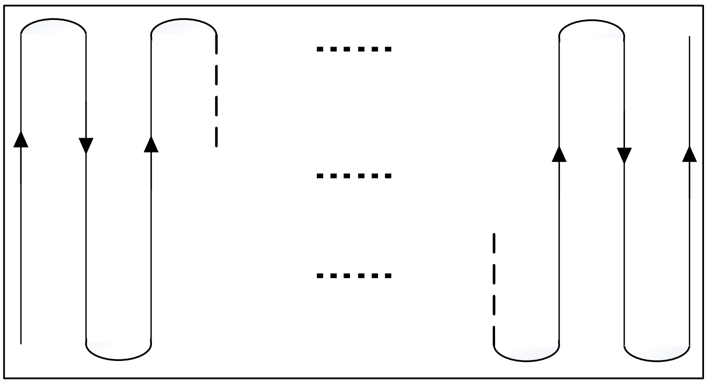

Figure 13. Tractor ploughing driving trajectory.

The average working speed is set to 5 km/h, the working time is 360 s, the starting time is 10 s and the average traction resistance value is 2500 N. The load demand power of the hybrid tractor under ploughing conditions is shown in Figure 14.

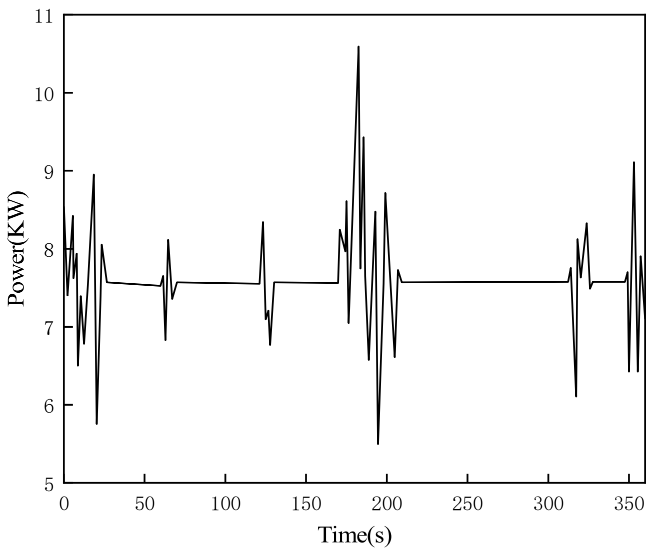

Figure 14. Typical ploughing conditions of tractors.

When the tractor ploughs, the load demand power is generally constant. When the tractor needs to turn around in the field, the load demand power fluctuates due to the change of traction resistance, and the maximum fluctuation range is ±3 KW.

4.2. Basic Parameter Settings

The design of the "FC + BT + SC" hybrid power system needs to meet the requirements of load demand power. The output power of the fuel cell needs to be greater than the average load power demand (7.5 KW). The lithium battery and supercapacitor provide continuous or instantaneous peak power demand compensation for the fuel cell, as shown in Table 3. In particular, in order to simplify the calculation, this paper does not consider the power consumption of auxiliary electrical equipment.

Table 3. Hybrid system simulation parameters.

	Parameter	Value
Fuel cell	Rated power/KW	10
	Peak power/KW	12.5
	Efficiency/%	50
	Power density/W · kg^{-1}	500
	Energy density/Wh · kg^{-1}	350
	Number of cells	65
Lithium battery	Rated capacity/Ah	40
	Rated voltage/V	48
	Rated discharge current/A	17
	Energy density/Wh · kg^{-1}	150
	Resistance/Ω	0.012
Supercapacitor	Rated voltage/V	290
	Rated capacitance/F	15.6
	Power density/KW · kg^{-1}	8900
	Energy density/Wh · kg^{-1}	5.5
	Resistance/Ω	0.15
DC/DC	Input voltage range/V	48–53
	Output voltage range/V	245–291
Motor	Rated power/KW	10
	Rated speed/r · min^{-1}	1500
	Rated torque/N · m	50

In addition, a 12.5 KW unidirectional DC/DC converter is equipped for the fuel cell, and a 4 KW bidirectional DC/DC converter is equipped for the lithium battery and supercapacitor, with an output voltage range of 150~300 V. The simulation model of the hybrid power system energy management strategy based on Matlab/Simulink established in this paper is shown in Figure 15:

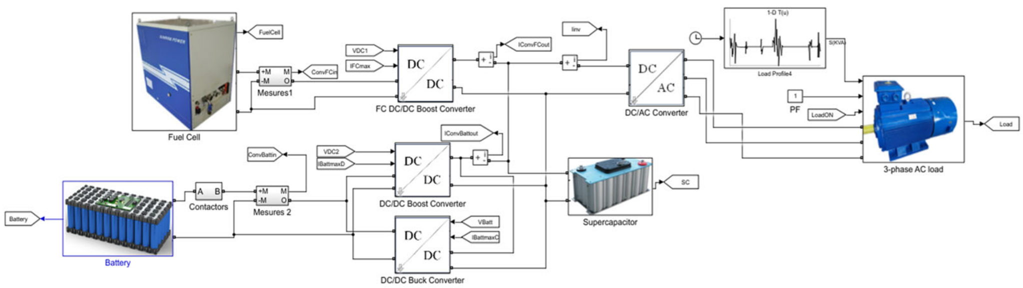

Figure 15. Simulation model of the hybrid system as a whole.

4.3. Analysis of Simulation Results

Based on the above simulation model and the designed tractor ploughing simulation condition, in the Matlab/Simulink simulation environment, the simulation time is 360 s, the initial SOC of the lithium battery is 70% and the initial voltage of the supercapacitor is 270 V. The SMC, ECMS and EEMS, three energy management strategies, are simulated and verified under the same initial conditions. The simulation results are as follows:

Figure 16 is the output power curve of the three power sources of the hybrid system under the SMC, ECMS and EEMS control strategies. It can be seen that in the initial stage, due to the slow dynamic response characteristics of the fuel cell, the additional power required for the load is immediately provided by the supercapacitor, and then the output power of the fuel cell is gradually increased to provide the main energy supply for the system, while the lithium battery plays a role of rapid response and power compensation for the fuel cell and recovery of braking energy when the tractor turns or the plowshare encounters the load power fluctuation caused by obstacles. Each control strategy can better meet the load power demand, and each power source works in the efficient working range, which ensures the stability of the hybrid system. The difference is that although the EEMS has a greater fluctuation in the output power of the fuel cell than the SMC and ECMS fuel cells, its fuel cell output burden is lighter, the continuous output power of the lithium battery and the supercapacitor is higher, the fuel consumption is smaller and the supercapacitor is fully utilized. The performance characteristics of absorbing transient load mutations reduce the risk of reduced service life of fuel cells and lithium batteries caused by load mutations, give full play to the advantages of hybrid power systems and ensure that the overall economy of the system is good during operation.

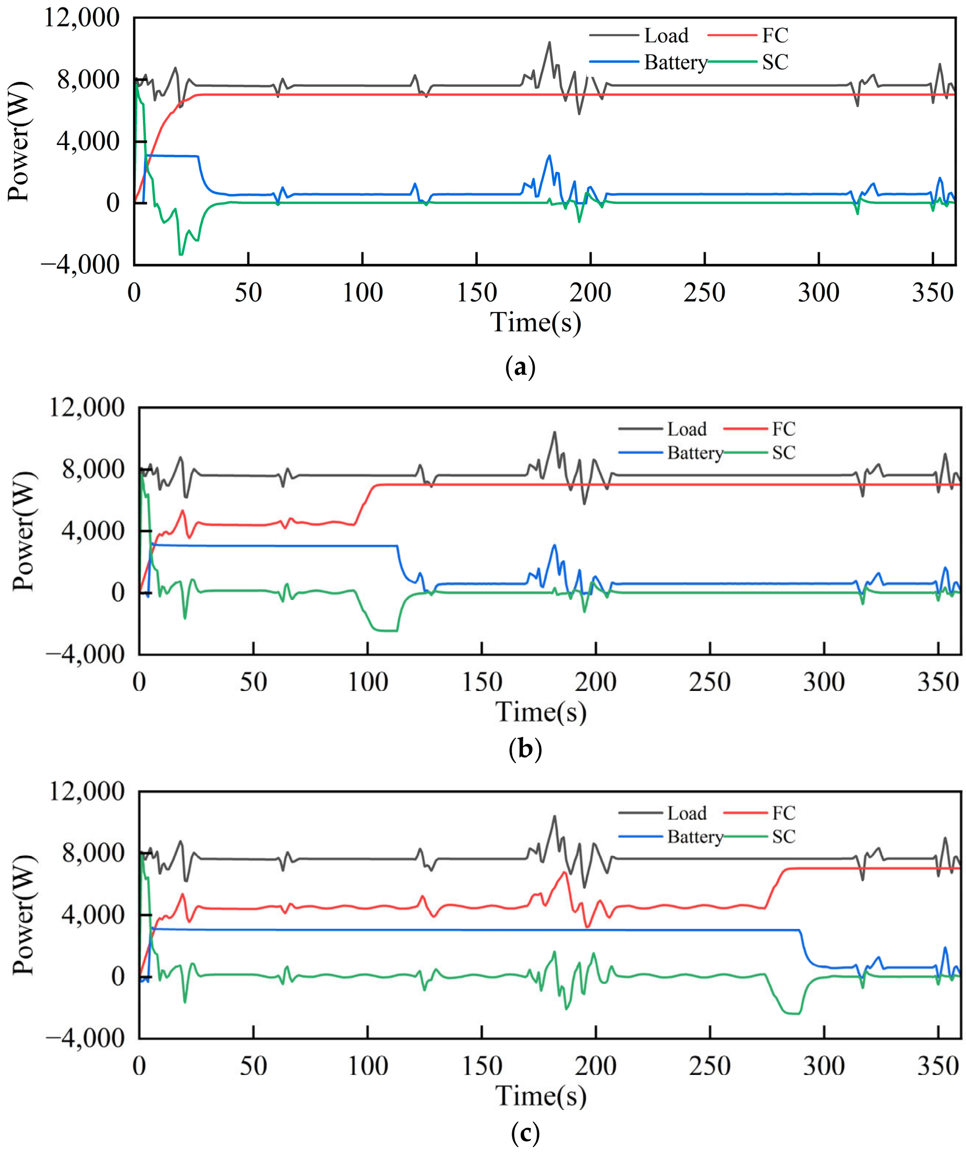

Figure 16. Output power and demand power of each power source under different strategies. (**a**) SMC. (**b**) ECMS. (**c**) EEMS.

Figures 17–19 show the current and voltage trends of fuel cells, supercapacitors and lithium batteries under the three control strategies. The average output voltage and current of each energy source are shown in Table 4.

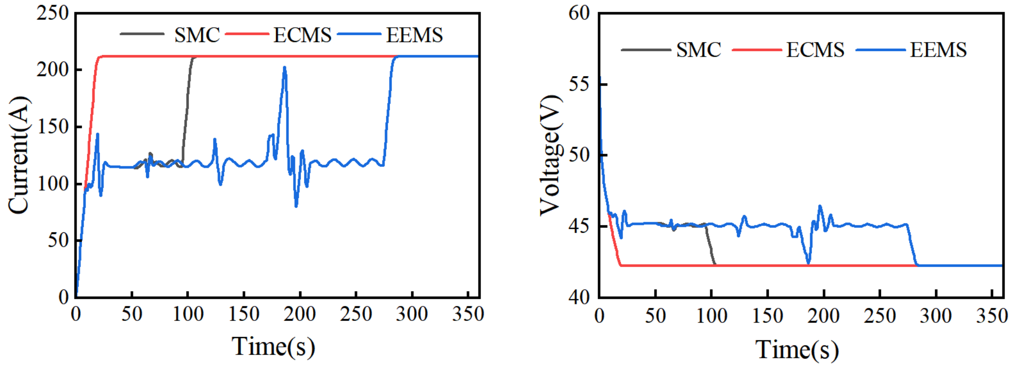

(**a**) (**b**)

Figure 17. Fuel cell output characteristics. (**a**) Current. (**b**) Voltage.

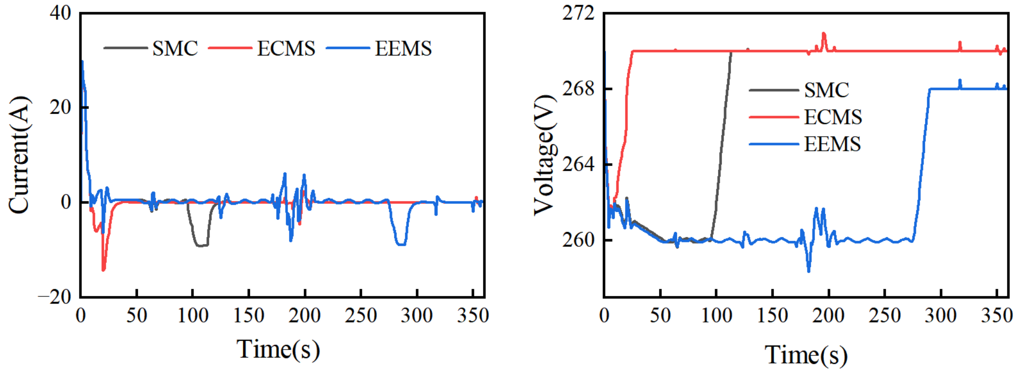

(**a**) (**b**)

Figure 18. Supercapacitor output characteristics. (**a**) Current. (**b**) Voltage.

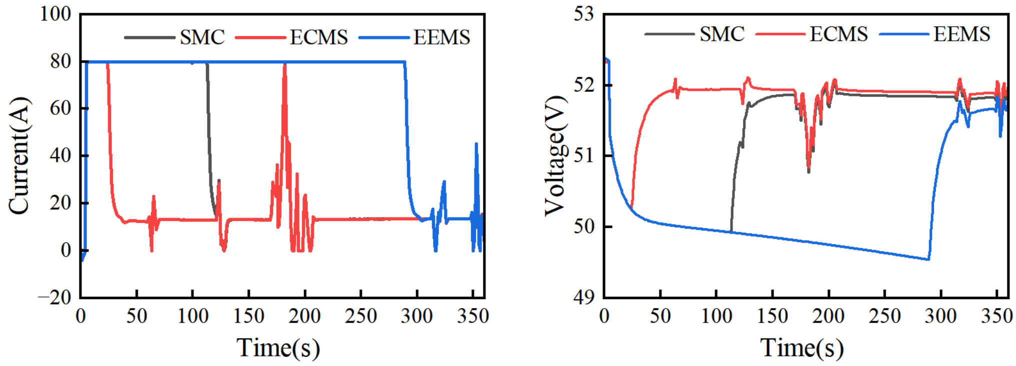

(**a**) (**b**)

Figure 19. Lithium battery output characteristics. (**a**) Current. (**b**) Voltage.

Table 4. The average output voltage and current of each power source are controlled by three strategies.

Parameter	EMS					
	SMC		ECMS		EEMS	
	Voltage/V	Current/A	Voltage/V	Current/A	Voltage/V	Current/A
Fuel cell	43.25	181.01	42.47	205.54	44.79	129.34
Supercapacitor	0.08	267.05	0.08	269.60	0.26	261.18
Lithium battery	36.19	51.23	18.23	51.79	72.50	50.05

As can be seen from Figure 17, under the control of SMC and ECMS, the fuel cell output current and voltage are stable at around 212 A and 42 V after the tractor starts, and the current varies between 0–213 A and the voltage varies between 42–212 V. Under the control of EEMS, the output current of the fuel cell fluctuates at about 120 A and the output voltage fluctuates at around 45 V after the tractor starts. Under the three control strategies, the output of the fuel cell is within the normal range, but the output state of the fuel cell will directly affect its service life, and the average output current of the fuel cell under the control of EEMS is 129.34 A, which is the smallest compared with the other two strategies, that is, the battery load is the least and the service life is the longest. As can be seen from Figure 18, the average output voltage of the supercapacitor under the control of EEMS is 0.26 V, which is the largest compared to the other two strategies, and the voltage and current fluctuations are also the largest, which means that the fuel cell and lithium battery are provided the most help, and their own performance characteristics are the most fully utilized. As can be seen from Figure 19, the average output voltage and current of the lithium battery under the control of EEMS are higher than those of the other two strategies, which is in line with the characteristics of maximizing the external energy efficiency and giving full play to the output performance of the lithium battery, and the output voltage of the lithium battery under the control of this strategy is near the nominal voltage, which is more efficient than the other two strategies.

At the same time, EEMS will also cause the lithium battery SOC to decline the fastest, as shown in Figure 20. At the end of a cycle, the final SOC value of a lithium battery under SMC and ECMS control decreases to about 56% and 60%, respectively, and the final value of the lithium battery SOC under EEMS control decreases to about 48%. Although the SOC of lithium batteries decreases the most under the control of EMMS, it still remains in the efficient operating range.

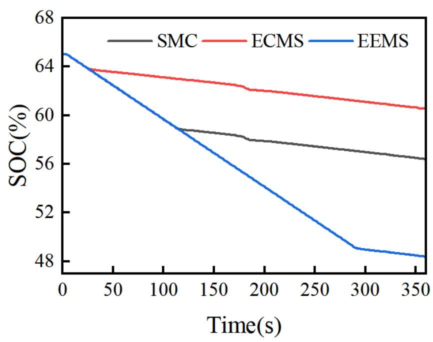

Figure 20. Lithium battery SOC changes.

Figure 21 shows the energy consumption of the three power sources of the tractor running for 360 s under different control strategies. It can be seen that the energy consumption of fuel cells under EEMS control is the smallest, while that of batteries and supercapacitors is the largest, which is in line with the objectives of the design strategy in this paper.

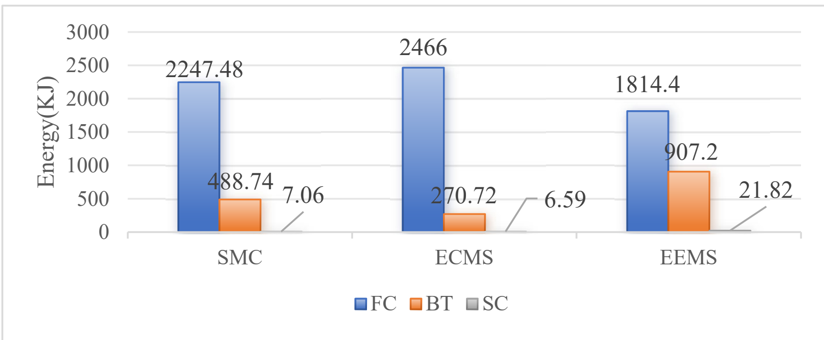

Figure 21. Three power sources' energy consumption.

The hydrogen consumption under the control of the three strategies is shown in Figure 22. The cumulative hydrogen consumption under EEMS control is significantly lower than that of SMC and ECMS, which is reduced by 11.03 g and 16.54 g, respectively, under one cycle condition. For a more in-depth comparison, the overall efficiency of the system is compared using the idea of the power conversion degree, which is defined as:

$$\eta_t = \frac{P_{load}}{P_{fc} + P_{bat} + P_{sc} + P_{equ}} \tag{28}$$

where P_{load} is load power; P_{fc}, P_{bat} and P_{sc} are the power input to fuel cells, lithium batteries and supercapacitors, respectively; P_{equ} is the power consumed by primary auxiliary equipment such as DC/DC converters.

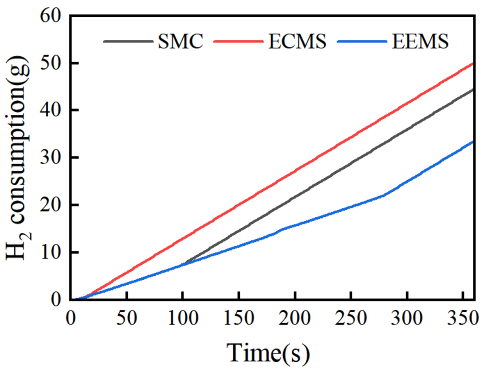

Figure 22. Total system hydrogen consumption.

After calculation, the electrical efficiency of the hybrid system under the control of the three strategies is 78.01%, 75.36% and 79.52%, respectively. Therefore, although the final SOC value of the lithium battery under the control of EEMS is lower, the system work efficiency is higher, the cumulative hydrogen consumption is less and the overall system economy is higher, which has obvious advantages over SMC and ECMS.

Based on the above simulation results, Table 5 shows the terminal simulation data of the three strategies of the hybrid system in terms of economy. It can be seen that, compared with the two traditional control strategies, the energy management strategy based on external energy efficiency maximization designed in this paper is more suitable for the tractor hybrid system in this paper, the overall operation of the hybrid system is stable in the ploughing operation conditions and the fuel economy is effectively improved, giving full play to the advantages of the hybrid system.

Table 5. The termination status of the three strategies under ploughing operations.

Parameter	EMS		
	SMC	**ECMS**	**EEMS**
Final SOC/%	56.39	60.52	48.38
H_2 consumption/g	44.60	50.11	33.57
Efficiency/%	78.01	75.36	79.52

5. Conclusions

In this paper, a hybrid drive scheme of "FC + BT + SC" suitable for tractors was designed by analyzing the output characteristics of multiple energy sources according to the complex and changeable working conditions of tractors. In this paper, an energy management strategy based on external energy efficiency maximization was designed with the optimization goal of minimizing equivalent hydrogen consumption, and the simulation and comparison analysis with the state machine and the energy management strategy with the minimum equivalent hydrogen consumption under typical ploughing conditions of tractors were obtained, and the conclusions are as follows:

Firstly, compared with the two traditional control strategies, EEMS can better adapt to the changing characteristics of tractor loads, giving full play to the output performance of the battery and the transient response characteristics of the supercapacitor, and the two auxiliary power sources share more pressure for the fuel cell and help improve the durability of the fuel cell.

Secondly, compared with the two traditional strategies, the overall efficiency of the proposed strategy system is increased by 1.51% and 4.16%, respectively, which ensures the efficient operation of the tractor hybrid system on the basis of satisfying the dynamics of the tractor. Hydrogen consumption was significantly reduced, and fuel economy was improved by 24% and 33%, respectively, proving the effectiveness of this strategy.

Finally, the current work is mainly based on model development and theoretical research, and the research results have certain scientific significance and reference value, but the accuracy of the experimental results needs to be verified, and the authenticity and reliability of the conclusions can be improved through specific experiments, which will be the focus of the next research work.

Author Contributions: Conceptualization, Z.G. and S.Z.; methodology, Z.G.; validation, Z.G. and X.L.; resources, S.Z. and Y.L.; project administration, L.X.; manuscript writing, Z.G.; image description, Z.G. and S.Z. All authors have read and agreed to the published version of the manuscript.

Funding: The National Key R&D Program of China (2022YFD2001203, 2022YFD2001201B); Key agricultural core technology research project (NK202216010103); 2022 Plan for Key Scientific Research Projects in Colleges and Universities of Henan Province (22B416001); Henan Province University Science and Technology Innovation Team Support Plan (24IRTSTHN029).

Institutional Review Board Statement: Not applicable.

Informed Consent Statement: Not applicable.

Data Availability Statement: The data presented in this study are available on request from the corresponding author. The data are not publicly available due to privacy.

Conflicts of Interest: The authors declare no conflicts of interest.

References

1. Algirdas, J.; Antanas, J.; Gediminas, P. Tractor's engine performance and emission characteristics in the process of ploughing. *Energy Convers. Manag.* **2013**, *75*, 498–508.
2. Editorial Department of China Energy. China Mobile Environmental Management Annual Report (2020) Released. *Energy China* **2020**, *42*, 47–50.
3. Chen, W.; Li, J. Review of agricultural tractor emissions. *South. Agric. Mach.* **2021**, *52*, 7–11.
4. Zhang, M. Thinking on Agricultural Mechanization Science and Technology Innovation: Historical Logic, Times Impact and Development Path. *Chin. J. Agric. Mech.* **2020**, *41*, 224–229.
5. Gorjian, S.; Fakhraei, O.; Gorjian, A.; Sharafkhani, A.; Aziznejad, A. Sustainable Food and Agriculture: Employment of Renewable Energy Technologies. *Curr. Robot. Rep.* **2022**, *3*, 153–163. [CrossRef] [PubMed]
6. Gao, Z.; Li, X.; Liu, Z. Research status and development trend of hydrogen fuel cell vehicles. *Mater. Rep.* **2022**, *36*, 70–77.
7. Zhang, Y. Research and thinking on hybrid use in tractor. *Agric. Eng. Technol.* **2021**, *41*, 56–57.
8. Chen, H. Optimal Management of Fuel Cell/Lithium Battery Hybrid System. Master's Thesis, Zhejiang University, Hangzhou, China, 2021.
9. Deng, T.; Huang, X. Research on Energy Management Strategy of Hybrid Electric Vehicle. *MATEC Web Conf.* **2015**, *22*, 03005. [CrossRef]
10. Ren, Y.; Zhong, Z.; Zhang, Z.; Luo, T. Continual Energy Management System of Proton Exchange Membrane Fuel Cell Hybrid Power Electric Vehicles. *MATEC Web Conf.* **2016**, *44*, 02019. [CrossRef]
11. Tan, Y.; Yang, D.; Zhang, C. Research on energy management of fuel cell hybrid system based on lithium-ion supercapacitor. *J. Jiamusi Univ. (Nat. Sci. Ed.)* **2019**, *37*, 236–239. [CrossRef]
12. He, H.; Meng, X. Review of energy management technology of hybrid electric vehicle. *J. Beijing Inst. Technol.* **2022**, *42*, 773–783. [CrossRef]
13. Yao, Y.; Zhou, Y. Overview of energy management strategy for hybrid vehicles based on rule strategy. *Times Mot.* **2023**, 10–12. [CrossRef]

14. Wang, T. Research on energy management strategy of fuel cell hybrid vehicle. *Henan Sci. Technol.* **2023**, *42*, 26–29. [CrossRef]
15. Truong, H.V.; Dao, H.V.; Do, T.C.; Ho, C.M.; To, X.D.; Dang, T.D.; Ahn, K.K. Mapping Fuzzy Energy Management Strategy for PEM Fuel Cell–Battery–Supercapacitor Hybrid Excavator. *Energies* **2020**, *13*, 3387. [CrossRef]
16. Peng, F.; Zhao, Y.; Li, X.; Liu, Z.; Chen, W.; Liu, Y.; Zhou, D. Development of master-slave energy management strategy based on fuzzy logic hysteresis state machine and differential power processing compensation for a PEMFC-LIB-SC hybrid tramway. *Appl. Energy* **2017**, *206*, 346–363. [CrossRef]
17. Wang, Z.; Luo, W.; Xu, S. Review of energy management strategies for fuel cell vehicles. *Battery* **2022**, *52*, 328–332. [CrossRef]
18. Dima, F.; Riad, C.; Ferdinand, P.; Sami, K.; Rabih, J. Dynamic programming technique for optimizing fuel cell hybrid vehicles. *Int. J. Hydrogen Energy* **2015**, *40*, 7777–7790.
19. Peng, H.; Chen, Z.; Li, J.; Deng, K.; Dirkes, S.; Gottschalk, J.; Ünlübayir, C.; Thul, A.; Löwenstein, L.; Pischinger, S. Offline optimal energy management strategies considering high dynamics in batteries and constraints on fuel cell system power rate: From analytical derivation to validation on test bench. *Appl. Energy* **2021**, *282*, 116152. [CrossRef]
20. Zhang, Q.; Tian, S.; Lin, X. Recent Advances and Applications of AI-Based Mathematical Modeling in Predictive Control of Hybrid Electric Vehicle Energy Management in China. *Electronics* **2023**, *12*, 445. [CrossRef]
21. Li, T.; Liu, H.; Wang, H.; Yao, Y. Hierarchical predictive control-based economic energy management for fuel cell hybrid construction vehicles. *Energy* **2020**, *198*, 117327. [CrossRef]
22. Li, X.; Han, L.; Liu, H.; Wang, W.; Xiang, C. Real-time optimal energy management strategy for a dual-mode power-split hybrid electric vehicle based on an explicit model predictive control algorithm. *Energy* **2019**, *172*, 1161–1178. [CrossRef]
23. Abdelqawee, I.M.; Emam, A.W.; ElBages, M.S. An improved energy management strategy for fuel cell/battery/supercapacitor system using a novel hybrid jellyfish/particle swarm/BAT optimizers. *J. Energy Storage* **2023**, *57*, 106276. [CrossRef]
24. Wang, S. Research on Energy Management Strategy of Fuel Cell Hybrid Electric Vehicle Based on Vehicle Speed Prediction. Master's Thesis, Jilin University, Changchun, China, 2023.
25. Motapon, S.N.; Lupien, B.A.; Dessaint, L.A.; Fortin, B.H.; Al, H.K. A Generic Electrothermal Li-ion Battery Model for Rapid Evaluation of Cell Temperature Temporal Evolution. *IEEE Trans. Ind. Electron.* **2017**, *64*, 998–1008. [CrossRef]
26. Hesham, A.; Hegazy, R.; Mohamed, L. Advanced Energy Management Strategy of Photovoltaic/PEMFC/Lithium-Ion Batteries/Supercapacitors Hybrid Renewable Power System Using White Shark Optimizer. *Sensors* **2023**, *23*, 1534.
27. Ye, Q. Research on Energy Management Strategy of Ship Fuel Cell Hybrid System. Master's Thesis, Jimei University, Xiamen, China, 2020.
28. Piraino, F.; Fragiacomo, P. A multi-method control strategy for numerically testing a fuel cell-battery-supercapacitor tramway. *Energy Convers. Manag.* **2020**, *225*, 113481. [CrossRef]
29. Zhang, H.; Yang, J.; Zhang, J. Optimal energy management of a fuel cell-battery-supercapacitor-powered hybrid tramway using a multi-objective approach. *Proc. Inst. Mech. Eng. Part F J. Rail Rapid Transit* **2020**, *234*, 511–523. [CrossRef]
30. Feng, H. Research on Energy Management Strategy of Fuel Cell Vehicle Based on Equivalent Hydrogen Consumption. Master's Thesis, Hefei University of Technology, Hefei, China, 2022.
31. Gao, F.; Zhang, H.; Wang, W. Energy-saving operation optimization of hydrogen fuel cell tram hybrid energy storage system. *Trans. China Electrotech. Soc.* **2022**, *37*, 686–696. [CrossRef]
32. Chen, X.; Guo, Y. Energy Management Optimization of Fuel Cell-Lithium Battery Hybrid Ships. *Ship Sci. Technol.* **2023**, *45*, 106–110. [CrossRef]
33. Njoya-Motapon, S.; Dessaint, L.A.; Al-Haddad, K. A comparative study of energy management schemes for a fuel-cell hybrid emergency power system of more-electric aircraft. *IEEE Trans. Ind. Electron.* **2014**, *61*, 1320–1334. [CrossRef]